

## Taylor & Francis Journals

Uncover Breakthroughs in Pharmaceutical Science and Medical Research with our Key Titles

Taylor and Francis

Open

## Journal of Oleo Science

### COUNTRY

Japan



Universities and research institutions in Japan



Media Ranking in Japan

### SUBJECT AREA AND CATEGORY

Chemical Engineering  
Chemical Engineering (miscellaneous)

Chemistry  
Chemistry (miscellaneous)

Medicine  
Medicine (miscellaneous)

### PUBLISHER

Japan Oil Chemists Society

### H-INDEX

51

### PUBLICATION TYPE

Journals

### ISSN

13473352, 13458957

### COVERAGE

2001-2022

### INFORMATION

[Homepage](#)

[How to publish in this journal](#)

[yukagaku@jocs-office.or.jp](mailto:yukagaku@jocs-office.or.jp)

**Submit pa  
for publica**

How to Publish Paper,  
free cost publication,  
ugc care journal policy...

X ⓘ IJNRC

Submit  
Paper for  
Publication

IJFMR - Academic Journal

IJFMR - Academic Journal

Open

**SCOPE**

The J. Oleo Sci. publishes original researches of high quality on chemistry, biochemistry and science of fats and oils such as related food products, detergents, natural products, petroleum products, lipids and related proteins and sugars. The Journal also encourages papers on chemistry and/or biochemistry as a major component combined with biological/sensory/nutritional/toxicological evaluation related to agriculture and/or food.

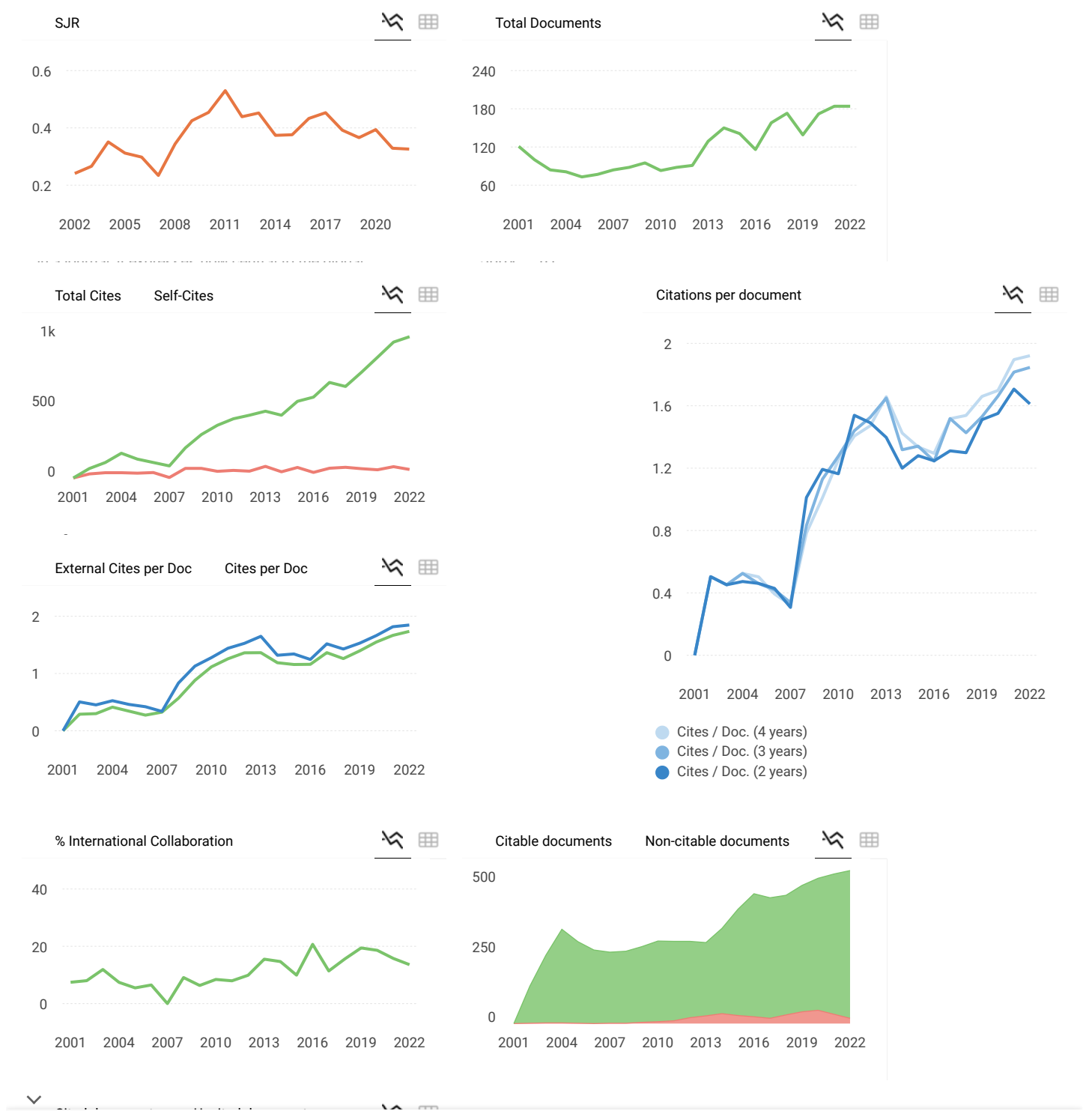
Join the conversation about this journal

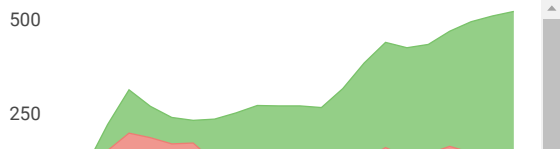
Quartiles



FIND SIMILAR JOURNALS ?

<p>1 <b>European Journal of Lipid Science and Technology</b> DEU</p> <p><b>62%</b> similarity</p>	<p>2 <b>JAOCs, Journal of the American Oil Chemists'</b> DEU</p> <p><b>55%</b> similarity</p>	<p>3 <b>Journal of Food Biochemistry</b> USA</p> <p><b>54%</b> similarity</p>	<p>4 <b>Grasas y Aceites</b> ESP</p> <p><b>5</b> si</p>
---	---	---	---





**Journal of Oleo Science**

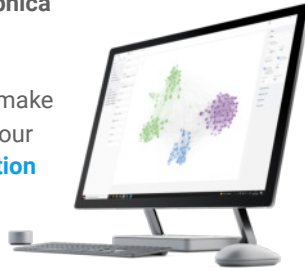
**Q3** Chemical Engineering (miscellaneous) best quartile

**SJR 2022** 0.33

powered by scimagojr.com

**SCImago Graphica**

Explore, visually communicate and make sense of data with our **new data visualization tool**.



Metrics based on Scopus® data as of April 2023



Loading comments...

Developed by:



Powered by:



Follow us on @ScimagoJR

Scimago Lab, Copyright 2007-2022. Data Source: Scopus®



[Cookie settings](#)

[Cookie policy](#)



# ZnO-Enhanced Reduced Graphene Oxide Electrodes from Cocoa Shell: Nanoarchitectonics Platform for Photoelectrocatalytic Detection of Methylene Blue

Thamrin Azis<sup>1\*</sup>, Muhammad Zakir Muzakkar<sup>1</sup>, Andi Tenri Nurwahida<sup>2</sup>, Nasriadi Dali<sup>1</sup>, La Ode Abdul Kadir<sup>1</sup>, Dian Ayu Lestari<sup>1</sup>, and La Ode Agus Salim<sup>3</sup>

<sup>1</sup> Department Chemistry, Faculty of Mathematics and Natural Sciences, Universitas Halu Oleo, Kendari 93231-Southeast Sulawesi, INDONESIA

<sup>2</sup> Department of Pharmacy, Faculty of Health and Pharmacy, Universitas Bani Saleh, Bekasi, 17113-West Java, INDONESIA

<sup>3</sup> Department of Chemistry, Faculty of Science Technology and Health, Institut Sains Teknologi dan Kesehatan (ISTEK) Aisyiyah Kendari, Kendari, 93116 – Southeast Sulawesi, INDONESIA

**Abstract:** In this study, we report the successful preparation of reduced graphene oxide modified zinc oxide (rGO-ZnO) composites from cocoa shells. Synthesis of rGO-ZnO was carried out using the Hummer method and thermal reduction. The electrode material was comprehensively characterized using fourier-transform infrared spectroscopy (FTIR), X-ray diffraction (XRD), and scanning electron microscopy & Energy Dispersive X-ray (SEM-EDX). The photoelectrocatalytic performance of the prepared composite electrodes was evaluated using various electrochemical techniques, including Linear Sweep Voltammetry (LSV), Cyclic Voltammetry (CV), and Multi Pulse Amperometry (MPA). The FTIR analysis of rGO-ZnO exhibited distinct bands corresponding to C-O at 1022 cm<sup>-1</sup>, C=C at 1600 cm<sup>-1</sup>, and Zn-O at 455 cm<sup>-1</sup>. The XRD analysis revealed characteristic peaks at 26.6°, 29.2°, 36.2°, 44.04°, 47.58°, and 64.4°, confirming the presence of key crystalline phases. SEM-EDX analysis of rGO-ZnO revealed a rough surface morphology with bright white and black regions, signifying the coexistence of ZnO and rGO with carbon, oxygen, and zinc contents of 78.98%, 17.46%, and 3.56%, respectively. The investigations involved the photoelectrochemical profiles of methylene blue organic dyes at different concentrations, ranging from 0.5 ppm to 3.0 ppm. The acquired findings offer valuable understanding into the photoelectrocatalytic effectiveness of the composite electrodes containing rGO-ZnO, suggesting their potential use in potential scenarios involving the revitalization of the environment in industrial water systems.

**Key words:** cocoa, rGO, ZnO, photoelectrocatalysis, methylene blue

## 1 Introduction

Methylene blue is a notable derivative of thiazine dye that has garnered significant attention as a potential solution for various environmental concerns. This compound exhibits remarkable properties and has found applications in diverse fields due to its distinct chemical structure and reactive characteristics<sup>1</sup>. Methylene blue can be sourced from multiple origins, including waste streams from industrial processes and textile dyeing operations. Its presence in these sources highlights the need for effective strategies to mitigate its impact on the environment<sup>2, 3</sup>. Understanding the properties and behavior of methylene blue is crucial in devising efficient methods for its removal and management.

In response to the challenges presented by pollution attributed to methylene blue, researchers have been motivated to develop cost-effective, environmentally friendly techniques for quantification and remediation of this substance. Among these techniques, electrochemical methods, specifically cyclic voltammetry (CV), have gained significant attention due to their rapid response times, exceptional sensitivity, and selectivity<sup>4-6</sup>. These methods provide real-time monitoring and accurate analysis of methylene blue concentrations across diverse matrices<sup>7, 8</sup>. Recent advancements in electrochemical sensor performance have been achieved through the integration of advanced nanomaterials. Among these materials, reduced graphene oxide (rGO), synthesized from cocoa shell waste,

\*Correspondence to: Thamrin Azis, Department Chemistry, Faculty of Mathematics and Natural Sciences, Universitas Halu Oleo, Kendari 93231-Southeast Sulawesi, INDONESIA

E-mail: thamrinazis006@gmail.com

Accepted August 30, 2023 (received for review August 12, 2023)

Journal of Oleo Science ISSN 1345-8957 print / ISSN 1347-3352 online

<http://www.jstage.jst.go.jp/browse/jos/> <http://mc.manuscriptcentral.com/jjocs>



has emerged as a promising candidate for electrode modification. Its distinctive structural and electrical properties render it an appealing platform for sensor development.

Cocoa husk, a byproduct of cocoa processing, presents environmental challenges owing to its disposal. Within this abundant cocoa shell lies considerable amounts of cellulose, lignin, and hemicellulose, with a substantial carbon content, rendering it suitable for the production of graphene oxide (GO)<sup>8, 9)</sup>. Both GO and graphene share a common graphene framework, exhibiting akin chemical, optical, and electrical properties<sup>10)</sup>. GO, enriched with functional groups like carboxylates, epoxy, carbonyl, hydroxyl, and phenolic groups, has found extensive application in diverse fields such as electrocatalysis, biomedical contexts, separation membranes, sensors, and energy conversion and storage<sup>11)</sup>.

Exploration has been undertaken to combine rGO with zinc oxide (ZnO) nanostructures, aiming to harness synergistic effects that yield improved conductivity and electrocatalytic activity<sup>12)</sup>. In the realm of photocatalytic reactions, ZnO acts as a semiconductor catalyst, particularly in waste treatment applications<sup>13)</sup>. ZnO boasts attributes such as non-corrosiveness, eco-friendliness, a high dielectric constant, abundance, stability, non-toxicity, and an energy gap of 3.37 eV with an excitation of 60 meV<sup>14)</sup>. However, its substantial band gap energy poses a limitation, confining its activity exclusively to UV light exposure and thereby curtailing its overall efficacy<sup>15)</sup>. To surmount these challenges and amplify photodegradation efficiency, integration of a supporting material becomes imperative to mitigate recombination rates and diminish the bandgap energy. A range of carbon-based materials, including carbon aerogel<sup>16)</sup>, carbon nanotubes<sup>17)</sup>, carbon dots<sup>18)</sup>, magnetic carbon<sup>19)</sup>, and GO<sup>20)</sup>, have been extensively researched to enhance the photocatalytic performance of ZnO nanoparticles.

Firstly, utilizing cocoa shell waste for producing reduced graphene oxide (rGO) brings economic and environmental benefits, transforming waste into valuable sensor material. Secondly, the synergy between rGO and zinc oxide (ZnO) enhances the electrocatalytic activity of the composite electrode better than ZnO or rGO electrodes alone. Thirdly, the rGO-ZnO composite exhibits improved visible light absorption compared to pure ZnO, holding potential for higher photoelectrocatalytic activity under sunlight. This study provides a comprehensive insight into the advantages of using rGO-ZnO composites derived from cocoa shell waste for photoelectrocatalytic applications.

Here we report the development of efficient and sustainable photocatalytic materials important to addressing pressing environmental challenges and advancing various technological applications. This research has several specific advantages, such as utilizing cocoa shell waste for producing rGO brings economic and environmental bene-

fits, transforming waste into valuable sensor material, the synergy between rGO and ZnO enhances the electrocatalytic activity and exhibits improved visible light absorption compared to pure ZnO, holding potential for higher photoelectrocatalytic activity under sunlight. The combination of rGO derived from cocoa shells with ZnO doping techniques presents a promising avenue for enhancing the photocatalytic activity of ZnO. By tuning the electronic band structure and improving visible light absorption, these doped ZnO materials hold great potential in the degradation of organic pollutants and the effective utilization of solar energy. This study aims to investigate the performance of the rGO cocoa composite electrode as a photoelectrocatalytic sensor for Methylene Blue, contributing valuable insights toward the development of innovative and sustainable solutions for environmental remediation and sensor applications. The mechanism for the performance enhancement of rGO-ZnO composite electrodes will be discussed.

## 2 Methods

### 2.1 Synthesis of rGO composite

The cocoa shells are subjected to a sun-drying process lasting 4-5 days, followed by their introduction into the combustion medium. The ensuing charcoal, derived from the combustion process, is subsequently comminuted and subjected to filtration using a 200-mesh pore size. The synthesis of GO entails the oxidation of graphite powders utilizing the Hummer modification method as delineated in reference<sup>21)</sup>. In this procedure, an initial amalgamation of 2.0 g of graphite (derived from cocoa shell charcoal) with 8 g of  $\text{KMnO}_4$ , 98 mL of concentrated  $\text{H}_2\text{SO}_4$ , and 4 g of concentrated  $\text{NaNO}_3$  facilitates an oxidative reaction that is maintained under stirring for a duration of 4 hours within an ice bath. The residual slurry generated thereafter is treated with 15 mL of  $\text{H}_2\text{O}_2$  solution, subsequent to its repeated washing with over 400 mL of deionized (DI) water, conducted iteratively (exceeding three cycles) until the solution reaches approximate neutrality (pH  $\sim 7$ ). Consecutively, the solution undergoes sequential washing with 0.1 M HCl, DI water, and alcohol, followed by multiple centrifugation steps, until nearing neutrality. Ultimately, the resultant product is subjected to vacuum oven drying at 60°C for a duration of 24 hours. All chemical substances employed in this procedure were bought from Aldrich (USA) and were employed directly without undergoing additional purification.

### 2.2 Preparation of rGO-ZnO composite electrode

The working electrode consists of a cylindrical glass with a diameter of 4 mm, which is connected to a copper wire. The preparation of the rGO-ZnO composite involved the simple mixing of ZnO with varying masses (0.1 g, 0.2 g, and

0.3 g) with 0.7 g of rGO. The resulting mixture was then ground and sieved using a 200-mesh stainless steel sieve. Subsequently, 0.3 g of paraffin oil was added, and the mixture was stirred for 30 minutes at a temperature of 80 °C. To ensure a smooth and flat surface, the electrode was polished with paper before conducting the experiment, yielding a glossy finish conducive to optimal electrochemical performance.

### 2.3 Characterization of composite

The composite chemical structure and size particle was assessed employing Fourier Transform Infrared spectroscopy (FTIR) on a Shimadzu IR Affinity-1S system and X-ray Diffraction (XRD) at  $2\theta = 10\text{-}70$  degrees using  $\text{Cu-K}\alpha = 1.54060$  on a Shimadzu 6000. The morphology and composition analysis of the rGO-ZnO composites was conducted through scanning electron microscopy & Energy Dispersive X-ray (SEM-EDX) using a HITACHI SU3500. Electrochemical properties investigation of the composite was carried out using cyclic voltammetry technique with a potentiostat DY2100. The electrochemical analysis utilized a glass container with a diameter of approximately 2.00 cm and a height of around 3.50 cm. The top cover of the container featured three holes to accommodate the electrodes, which included the working and auxiliary electrodes, along with a reference electrode.

### 2.4 Photoelectrocatalytic degradation of methylene blue

The investigation pertained to the photoelectrocatalytic degradation of methylene blue and was conducted within a three-electrode electrochemical configuration. In this arrangement, the working electrode was fabricated employing rGO-ZnO composite material, a depiction of which is presented in Fig. 1. The reference electrode of choice encompassed an Ag/AgCl configuration, while the counter electrode consisted of a Pt plate. Multi-Pulse Amperometry (MPA) was the elected technique for experimentation,

wherein a potential bias of 0.5 V was maintained. The illumination source encompassed a 15-watt UV lamp radiating light at a wavelength of 360 nm, accompanied by visible light irradiation at an energy level of 18 Watts, facilitated by a Xenon lamp. The experimental conditions dictated that the photochemical reactor system sustain ambient room temperature. The protocol entailed treating 2.0 mL of methylene blue dye at ten-minute intervals, spanning a total experimental duration of 1 hour. Monitoring of the degradation process was executed through employment of a UV-Vis spectrometer. Parallel experimentation adhering to identical conditions was executed utilizing a rGO electrode, serving as a reference point for comparison.

## 3 Results and Discussion

### 3.1 Characterization of rGO-ZnO electrode

The FTIR characterization of the (rGO-ZnO) electrode aimed to identify functional groups formed during synthesis. The presence of these groups was determined through transmittance peaks in the FTIR spectrum ( $4000\text{ cm}^{-1}$  to  $400\text{ cm}^{-1}$ ). Figure 2 shows the FTIR results for the (rGO-ZnO) electrode, indicating distinctive absorption peaks. Notably, peaks at  $3390\text{ cm}^{-1}$ ,  $1710\text{ cm}^{-1}$ ,  $1600\text{ cm}^{-1}$ , and  $1024\text{ cm}^{-1}$  were attributed to the O-H, C-O, C-C, and C-O bonds, respectively<sup>22</sup>. Moreover, the FTIR analysis identified a ZnO bond at  $455\text{ cm}^{-1}$  in the rGO-ZnO composite. For the rGO sample prepared via thermal reduction, the FTIR spectra exhibited vibrational peaks at  $455\text{ cm}^{-1}$  (confirming Zn-O bonds) and  $1600\text{ cm}^{-1}$  (C=C bond) and  $1024\text{ cm}^{-1}$  (C-O bond) characteristic of rGO. Interestingly, the FTIR analysis did not show any vibration related to the O-H group in the rGO-ZnO composite. This can be attributed to the thermal reduction method, which avoids water use at high temperatures, preventing the formation of O-H groups. These FTIR results align with prior studies on rGO-

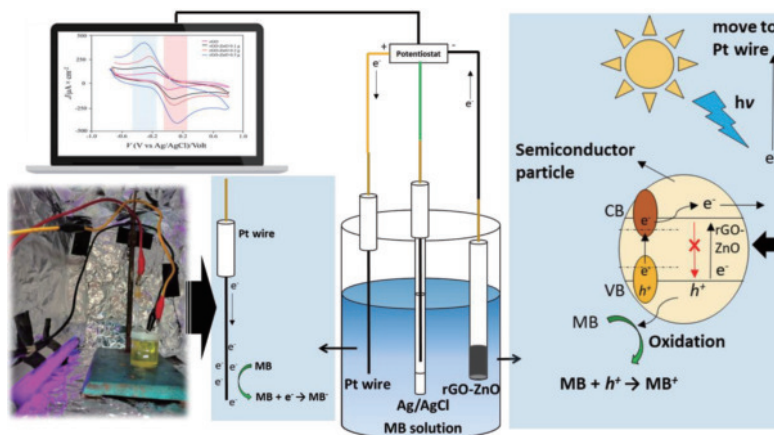


Fig. 1 Visual representation of the working electrode structure, specifically the rGO-ZnO electrode, through photoelectrochemical experiments.



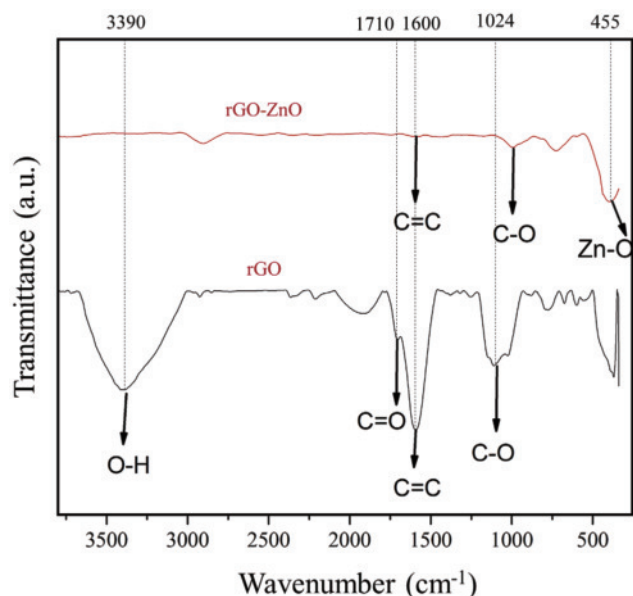


Fig. 2 shows the results of FTIR analysis for rGO.

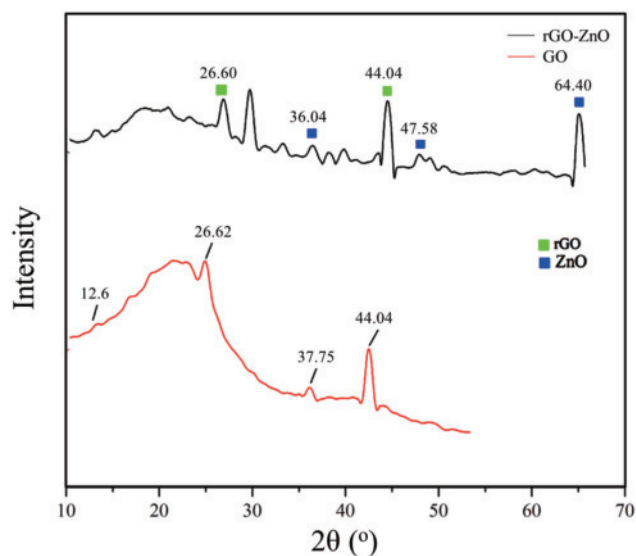


Fig. 3 XRD spectra of GO and rGO-ZnO.

based composites<sup>22</sup>, further validating the synthesis and characterization approach.

The phases present in the material were determined through XRD analysis. Figure 3 displays the XRD results of both GO and rGO-ZnO. The XRD patterns of the GO crystals exhibit distinct diffraction peaks at approximately  $2\theta = 12.6^\circ, 26.62^\circ, 37.75^\circ,$  and  $44.04^\circ$ , with corresponding interlayer spacings ( $d$ ) of 0.984 Å, 3.345 Å, 2.381 Å, and 2.054 Å, respectively. Notably, the characteristic  $2\theta$  band at  $10\text{--}12^\circ$  is unique to GO. The XRD analysis provides valuable insights into the crystal structures and phases present in the material. The prominent peaks observed in the XRD patterns indicate the presence of specific crystal planes and interlayer spacing within GO and rGO-ZnO. Moreover, the

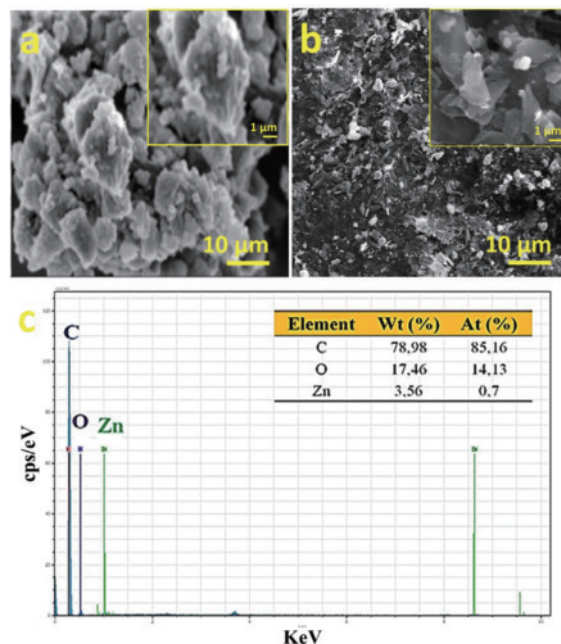


Fig. 4 Morphological and compositional characteristics illustrated. SEM depiction (a) rGO, (b) rGO-ZnO, along with EDX analysis results (c) for rGO-ZnO.

XRD data helps to validate the successful reduction of GO to rGO and the incorporation of ZnO into the composite material. These XRD results are consistent with previous studies on GO-based composites<sup>23</sup>, further supporting the identification of crystal phases and lattice parameters within the material.

The SEM images revealed elements like rGO tend to absorb light, resulting in darker-colored particles Fig. 4a. Distinct features of transparent black and bright white particles, corresponding to rGO and ZnO particles, respectively (Fig. 4b). This phenomenon can be attributed to the metallic nature of ZnO, leading to a brighter appearance when exposed to light. Additionally, the irregular morphological shape of the ZnO compound was observed, as reported in previous studies<sup>24</sup>. Further quantitative analysis of the rGO-ZnO composites elemental composition was carried out through Energy Dispersive X-ray Spectroscopy (EDX), as depicted in Fig. 4c. The EDX spectra of incorporation of rGO into the ZnO powder confirmed the presence of carbon (C), oxygen (O), and zinc (Zn) contents of 78.98%, 17.46%, and 3.56%, respectively. The SEM and EDX characterizations provide essential insights into the morphology and elemental composition of the rGO-ZnO electrode composite. These findings support the successful synthesis and doping of rGO in the ZnO matrix, validating the composite's structural integrity and composition. These results are consistent with previous research on similar rGO-ZnO composites<sup>25</sup>, further corroborating the characterization outcomes and supporting the composite's potential for



various applications.

### 3.2 $\text{Fe}(\text{CN})_3^{-6}/\text{Fe}(\text{CN})_4^{-6}$ electrochemical system

The present method focuses on the electrochemical behavior of four different working electrodes in the presence of  $\text{K}_3[\text{Fe}(\text{CN})_6]$  as the electrolyte solution. From the obtained CV graphs, distinct peak potentials, and peak currents were observed for each electrode. For the rGO electrode, a cathodic peak potential ( $E_{pc}$ ) of 0.06 V and an anodic peak potential ( $E_{pa}$ ) of  $-0.25$  V were recorded, with corresponding cathodic peak current ( $I_{pc}$ ) of  $-68 \mu\text{A}$  and anodic peak current ( $I_{pa}$ ) of  $99 \mu\text{A}$ . The introduction of ZnO into the rGO matrix resulted in notable changes in the electrochemical behavior. The rGO-ZnO composite with 0.1 gram of ZnO displayed a cathodic peak potential ( $E_{pc}$ ) of 0.02 V and an anodic peak potential ( $E_{pa}$ ) of 0.29 V, accompanied by cathodic peak current ( $I_{pc}$ ) of  $-163 \mu\text{A}$  and anodic peak current ( $I_{pa}$ ) of  $165 \mu\text{A}$ . As the ZnO content increased to 0.2 grams, the composite exhibited a cathodic peak potential ( $E_{pc}$ ) of 0.03 V and an anodic peak potential ( $E_{pa}$ ) of  $-0.31$  V, with cathodic peak current ( $I_{pc}$ ) of  $-226 \mu\text{A}$  and anodic peak current ( $I_{pa}$ ) of  $266 \mu\text{A}$ . Further increasing the ZnO content to 0.3 grams resulted in a cathodic peak potential ( $E_{pc}$ ) of 0.06 V and an anodic peak potential ( $E_{pa}$ ) of  $-0.38$  V, with cathodic peak current ( $I_{pc}$ ) of  $-414 \mu\text{A}$  and anodic peak current ( $I_{pa}$ ) of  $402 \mu\text{A}$ .

These observations indicate that the incorporation of ZnO significantly influences the electrochemical behavior of the rGO-ZnO composite (Fig. 5). The variations in peak potentials and peak currents suggest changes in the redox kinetics and charge transfer processes within the composite materials. The presence of ZnO may alter the electron transport pathways and affect the overall electrochemical performance of the composite. The findings from this study shed light on the potential applications of rGO-ZnO composites in various electrochemical devices, including sensors, batteries, and supercapacitors<sup>26)</sup>. The ability to tune the electrochemical behavior by varying the ZnO content provides a means to tailor the composite's properties for specific applications<sup>27)</sup>. Further investigation and optimization of rGO-ZnO composites may lead to enhanced electrochemical performance and expanded functionalities in future electrochemical technologies. However, more in-depth analysis and comprehensive characterization techniques are warranted to fully understand the underlying mechanisms and optimize the performance of these materials.

### 3.3 Photoelectrocatalytic performance

Figure 6a presents the ZnO activity under different light irradiation conditions, showing the highest activity with UV light, indicative of strong photoelectrocatalysis. However, visible light and dark conditions resulted in comparatively lower ZnO activity due to less absorbability by the ZnO

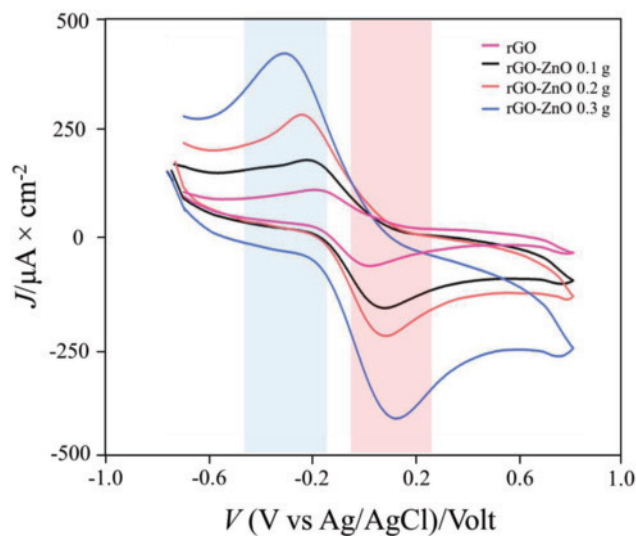


Fig. 5 The CV graph by comparing four working electrodes using  $\text{K}_3[\text{Fe}(\text{CN})_6]$  as an electrolyte solution.

working electrode caused by larger visible light wavelength. In the absence of light, the ZnO working electrode failed to facilitate the necessary energy transfer between conduction and valence bands. Meanwhile, Fig. 6b illustrates the photoelectrocatalysis activities of the rGO-ZnO electrode, exhibiting efficient photoelectrocatalysis under visible light irradiation. These results underscore the importance of light wavelength in designing effective photoelectrocatalytic systems and call for further investigations to optimize the performance and understand the underlying mechanisms of these materials<sup>28)</sup>.

Photocurrent response measurement of rGO-ZnO electrodes to methylene blue compounds was carried out using the MPA method. Based on Fig. 6c the photocurrent produced from MB dye solution is greater than that of the electrolyte solution. The resultant photocurrent comprises the combined oxidation currents of both methylene blue compounds and the electrolyte solutions<sup>29)</sup>. The existence of this electrolyte solution enhances the conductivity of the solution, and this conductivity is directly linked to the intensity of the light-induced current. According to<sup>30)</sup>, the photocurrent in the solution containing the analyte is expected to match the photocurrent of the blank solution when the degradation process is finished. Nevertheless, the figure depicted above doesn't display the analyte's photocurrent curve aligning with the blank solution's photocurrent. This discrepancy can be attributed to the excessive volume of the methylene blue compound solution, preventing the oxidation process from completing within the 60-second timeframe.

The relationship between  $Q_{\text{net}}$  (net charge) and the concentration of methylene blue compounds was investigated, as depicted in Fig. 7. The primary objective was to

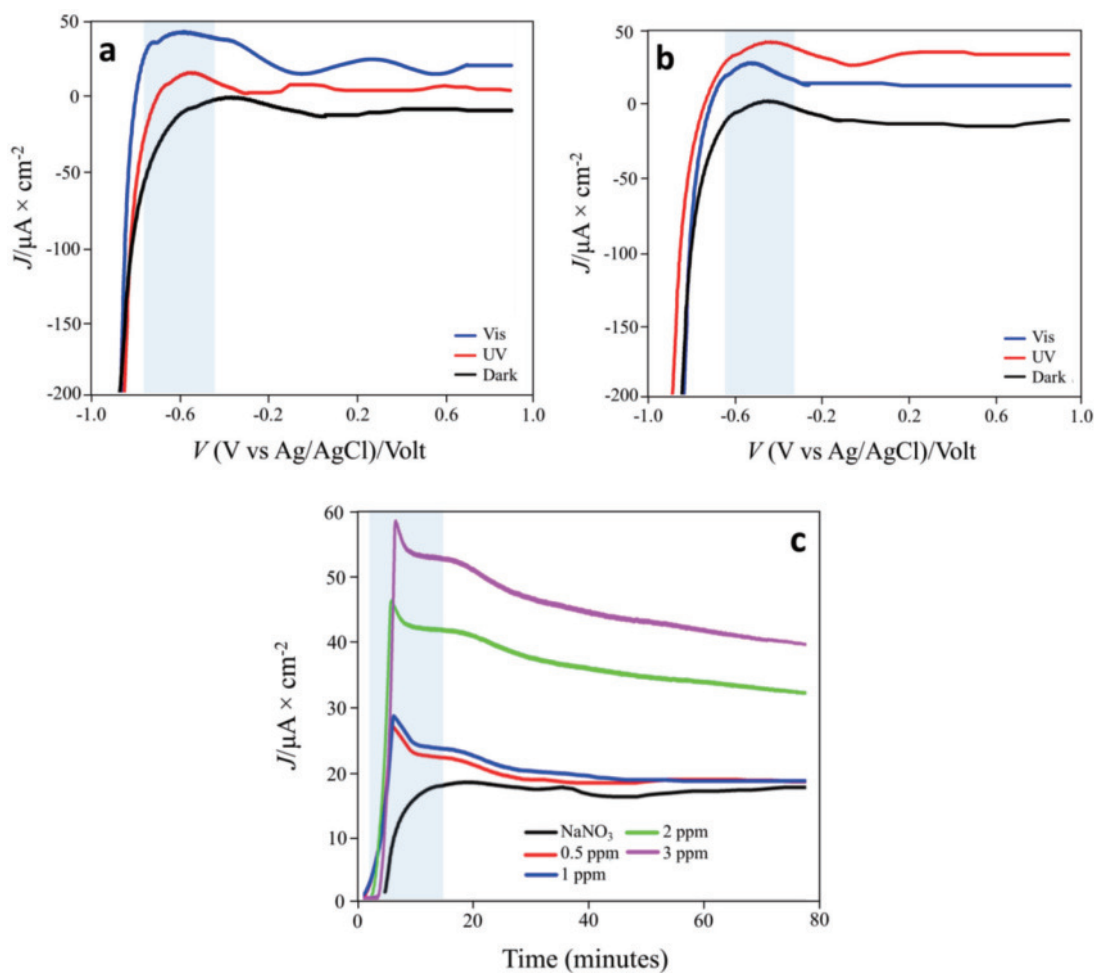


Fig. 6 The LSV graph(a) ZnO electrode, (b) rGO-ZnO electrode, and (c) amperomogram of rGO-ZnO electrode.

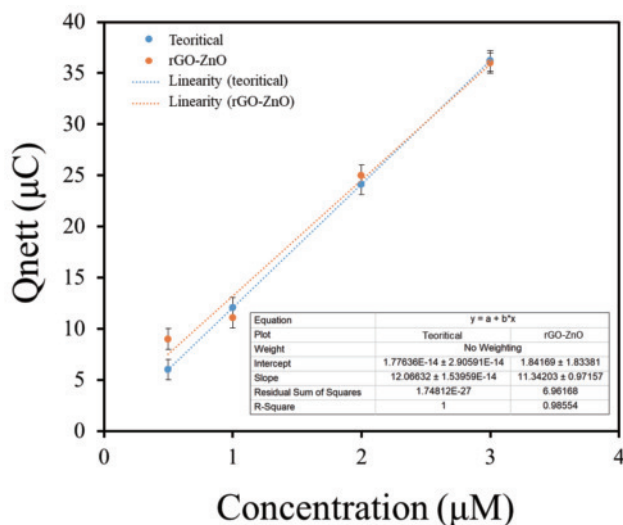


Fig. 7 The relation between  $Q_{nett}$  and concentration methylene blue compound.

evaluate the performance of the rGO-ZnO electrode in detecting methylene blue compounds, by comparing the generated charge value with the theoretical charge value. The results reveal that the rGO-ZnO electrode exhibits exceptional precision in detecting methylene blue compounds. This remarkable precision is in accordance with Faraday's law, a fundamental principle in electrochemistry, which states that the amount of charge produced during an electrochemical reaction is directly proportional to the quantity of substance undergoing oxidation or reduction at the electrode. Hence, as the concentration of methylene blue compounds in the solution increases, the charge reception at the electrode also increases<sup>31</sup>.

The observed precision in detecting MB dye compounds can be attributed to the strong interaction between the catalyst's surface and the organic compounds. This interaction promotes a higher rate of oxidation for the methylene blue molecules, resulting in a greater generation of electric charge<sup>31, 32</sup>. The efficient oxidation process further corroborates the electrode's proficiency in handling methylene blue compounds. The empirical evidence obtained in this

study significantly strengthens the understanding of the rGO-ZnO electrode's effectiveness as a sensor for MB compounds. These findings have implications for the development of advanced electrochemical sensors and may find applications in environmental monitoring, water quality assessment, and other fields where the detection of organic compounds is of paramount importance. However, further research and validation are warranted to explore the electrode's performance under varying experimental conditions and to investigate its potential for practical applications in real-world scenarios.

#### 4 Conclusion

In this study, we successfully prepared rGO-ZnO composite electrodes from cocoa shell. The synthesis of rGO-ZnO was conducted using the Hummer method and thermal reduction. FTIR analysis of rGO-ZnO showed distinct bands corresponding to C-O at  $1022\text{ cm}^{-1}$ , C=C at  $1600\text{ cm}^{-1}$ , and Zn-O at  $455\text{ cm}^{-1}$ . XRD analysis revealed characteristic peaks at  $26.6^\circ$ ,  $29.2^\circ$ ,  $36.2^\circ$ ,  $44.04^\circ$ ,  $47.58^\circ$ , and  $64.4^\circ$ , confirming the presence of key crystalline phases. SEM-EDX analysis of rGO-ZnO revealed a rough surface morphology with bright white and black regions, signifying the coexistence of ZnO and rGO with carbon, oxygen, and zinc contents of 78.98%, 17.46%, and 3.56%, respectively. The investigation involved photoelectrochemical profiles of methylene blue organic dyes at different concentrations, ranging from 0.5 ppm to 3.0 ppm. The obtained results provide valuable insights into the photoelectrocatalytic efficiency of the rGO-ZnO composite electrodes for potential applications in environmental restoration within industrial water systems.

#### Author Contributions

T.A. and D.A.L. performed all the experiments. T.A. coordinated the study. M.Z.M. contributed the analytic tools. L.O.A.S. and A.T.N. writing the manuscript. N.D. and L.O.A.K. processed the research data. All authors have read and agreed to the published version of the manuscript.

#### Acknowledgment

We acknowledge the financial support from the Ministry of Education, Culture, Research and Technology of the Republic of Indonesia under the Fundamental Research award grant no. DIPA-023.17.1.690523/2023.

#### Conflict of Interest Statement

The authors declare that we have no competing financial interests or personal relationships that could have appeared to influence the work reported in this paper.

#### References

- 1) Oladoye, P.O.; Ajiboye, T.O.; Omotola, E.O.; Oyewola, O.J. Methylene blue dye: Toxicity and potential elimination technology from wastewater. *Results Eng.* **16**, 100678 (2022).
- 2) Raheb, I.; Manlla, M.S. Kinetic and thermodynamic studies of the degradation of methylene blue by photo-Fenton reaction. *Helvion* **7**, 6 (2021).
- 3) Harris, J.; Silk, R.; Smith, M.; Dong, Y.; Chen, W.T.; Waterhouse, G.I.N. Hierarchical  $\text{TiO}_2$  nanoflower photocatalysts with remarkable activity for aqueous methylene blue photo-oxidation. *ACS Omega* **7**, 5 (2020).
- 4) Nurdin, M.; Ritonga, H.; Astria, M.; Salim, L.O.A.; Annisa, D.; Maulidiyah, M. Photocatalytic sensor for chemical oxygen demand flow system using N-TiO<sub>2</sub>/Ti electrode: Determination of glucose and potassium hydrogen phthalate. *J. Phys. Conf. Ser.* **1899**, 012040 (2021).
- 5) Nurdin, M.; Arham, Z.; Rasyid, J.; Maulidiyah, M.; Mustapa, F. *et al.* Electrochemical performance of carbon paste electrode modified  $\text{TiO}_2/\text{Ag-Li}$  (CPE-TiO<sub>2</sub>/Ag-Li) in determining fipronil compound. *J. Phys. Conf. Ser.* **1763**, 012067 (2021).
- 6) Nurdin, M.; Maulidiyah, M.; Watoni, A.H.; Armawansa, A.; Salim, L.O.A. *et al.* Nanocomposite design of graphene modified  $\text{TiO}_2$  for electrochemical sensing in phenol detection. *Korean J. Chem. Eng.* **39**, 209-215 (2022).
- 7) Wibowo, D.; Malik, R.H.A.; Mustapa, F.; Nakai, T.; Maulidiyah, M.; Nurdin, M. Highly synergistic sensor of graphene electrode functionalized with rutile  $\text{TiO}_2$  microstructures to detect l-tryptophan compound. *J. Oleo Sci.* **71**, 759-770 (2022).
- 8) Azis, T.; Maulidiyah, M.; Muzakkar, M.Z.; Ratna, R.; Aziza, S.W. *et al.* Examination of carbon paste electrode/ $\text{TiO}_2$  nanocomposite as electrochemical sensor for detecting profenofos pesticide. *Surf. Eng. Appl. Electrochem.* **57**, 387-396 (2021).
- 9) Qureshi, D.; Choudhary, B.; Mohanty, B.; Sarkar, P.; Anis, A. *et al.* Graphene oxide increases corneal permeation of ciprofloxacin hydrochloride from oleogels: A study with cocoa butter-based oleogels. *Gels* **6**, 4 (2020).
- 10) Xu, J.; Lu, L.; Duan, G.; Zhao, W. Characteristic analysis of three-ecofriendly reduced graphene oxides (rGOs) and their application in water-ethanol-based fluids with different volume ratios. *RSC Adv.* **12**, 9

- (2022).
- 11) Qian, L.; Thirupathi, A.R.; Elmahdy, R.; Zalm, J.V.D.; Chen, A. Graphene-oxide-based electrochemical sensors for the sensitive detection of pharmaceutical drug naproxen. *Sensors* **20**, 5 (2020).
  - 12) Boukhoubza, I.; Khenfouch, M.; Achehboune, M.; Mothudi, B.M.; Zorkani, I.; Jorio, A. Graphene oxide/ZnO nanorods/graphene oxide sandwich structure: The origins and mechanisms of photoluminescence. *J. Alloys Compd.* **797**, 1 (2019).
  - 13) Cardoza-Contreras, M.N.; Vásquez-Gallegos, A.; Vidal-Limon, A.; Romo-Herrera, J.M.; Águila, S.; Contreras, O.E. Photocatalytic and antimicrobial properties of Ga doped and Ag doped ZnO nanorods for water treatment. *Catalysts* **9**, 2 (2019).
  - 14) Pramanik, S.; Mondal, S.; Mandal, A.C.; Mukherjee, S.; Das, S. *et al.* Role of oxygen vacancies on the green photoluminescence of microwave-assisted grown ZnO nanorods. *J. Alloys Compd.* **849**, 1 (2020).
  - 15) Lin, C.J.; Liao, S.J.; Kao, L.C.; Liou, S.Y.H. Photoelectrocatalytic activity of a hydrothermally grown branched ZnO nanorod-array electrode for paracetamol degradation. *J. Hazard. Mater.* **291**, 9-17 (2015).
  - 16) Ngullie, R.C.; Bhuvaneswari, K.; Shanmugam, P.; Boonyuen, S.; Smith, S.M.; Sathishkumar, M. Magnetically recoverable biomass-derived carbon-aerogel supported ZnO (ZnO/MNC) composites for the photodegradation of methylene blue. *Catalysts* **12**, 9 (2022).
  - 17) Naeimi, A.; Khoshkam, S.; Eslaminejad, T. Natural cellulose fibers from Quinoa wastes reinforced carbon nanotube/ZnO bio-nanocomposite as a novel recyclable catalyst for oxidation reaction. *Polym. Bull.* **79**, 9 (2022).
  - 18) Pangajam, A.; Theyagarajan, K.; Dinakaran, K. Highly sensitive electrochemical detection of *E. coli* O157:H7 using conductive carbon dot/ZnO nanorod/PANI composite electrode. *Sens. Bio-Sensing Res.* **29**, 100317 (2020).
  - 19) Wang, Y.F.; Shao, Y.C.; Hsieh, S.H.; Chang, Y.K.; Yeh, P.H. *et al.* Origin of magnetic properties in carbon implanted ZnO nanowires. *Sci. Rep.* **8**, 1 (2018).
  - 20) Zhong, L.; Yun, K. Graphene oxide-modified ZnO particles: Synthesis, characterization, and antibacterial properties. *Int. J. Nanomedicine* **10**, 79-92 (2015).
  - 21) Nurdin, M.; Agus, L.; Putra, A.A.M.; Maulidiyah, M.; Arham, Z. *et al.* Synthesis and electrochemical performance of graphene-TiO<sub>2</sub>-carbon paste nanocomposites electrode in phenol detection. *J. Phys. Chem. Solids* **131**, 104-110 (2019).
  - 22) Irwan, I.; Jumbi, I.S.; Alimin, A.; Ratna, R.; Nohong, N. *et al.* Electrochemical photodegradation of methyl red using reduction graphene oxide of palm shells supported TiO<sub>2</sub> nanoparticle under visible irradiation. *Anal. Bioanal. Electrochem.* **15**, 556-567 (2023).
  - 23) Kumar, M.I.S.; Kirupavathy, S.S.; Jerusha, E.; Sureshkumar, S.; Vinolia, M. Synthesis and characterization of novel reduced graphene oxide supported barium niobate (RGOBN) nanocomposite with enhanced ferroelectric properties and thermal stability. *J. Mater. Sci. Mater. Electron.* **29**, 19228-19237 (2018).
  - 24) Muhammad, W.; Ullah, N.; Haroon, M.; Abbasi, B.H. Optical, morphological and biological analysis of zinc oxide nanoparticles (ZnO NPs) using: *Papaver somniferum* L. *RSC Adv.* **9**, 51 (2019).
  - 25) Elbasuney, S.; El-Sayyad, G.S.; Tantawy, H.; Hashem, A.H. Promising antimicrobial and antibiofilm activities of reduced graphene oxide-metal oxide (RGO-NiO, RGO-AgO, and RGO-ZnO) nanocomposites. *RSC Adv.* **11**, 25961-25975 (2021).
  - 26) Buldu-Akturk, M.; Toufani, M.; Tufani, A.; Erdem, E. ZnO and reduced graphene oxide electrodes for all-in-one supercapacitor devices. *Nanoscale* **14**, 3269-3278 (2022).
  - 27) Hao, J.; Ji, L.; Wu, K.; Yang, N. Electrochemistry of ZnO@reduced graphene oxides. *Carbon* **130**, 480-486 (2018).
  - 28) Maulidiyah, M.; Azis, T.; Nurwahidah, A.T.; Wibowo, D.; Nurdin, M. Photoelectrocatalyst of Fe co-doped N-TiO<sub>2</sub>/Ti nanotubes: pesticide degradation of thiamethoxam under UV-visible lights. *Environ. Nanotechnol. Monit. Manag.* **8**, 103-111 (2017).
  - 29) Gholivand, M.B.; Ahmadi, E.; Haseli, M. A novel voltammetric sensor for nevirapine, based on modified graphite electrode by MWCNs/poly(methylene blue)/gold nanoparticle. *Anal. Biochem.* **527**, 4-12 (2017).
  - 30) Wibowo, D.; Muzakkar, M.Z.; Saad, S.K.M.; Mustapa, F.; Maulidiyah, M. *et al.* Enhanced visible light-driven photocatalytic degradation supported by Au-TiO<sub>2</sub> coral-needle nanoparticles. *J. Photochem. Photobiol. A* **398**, 112589 (2020).
  - 31) Nurdin, M.; Muzakkar, M.Z.; Maulidiyah, M.; Trisna, T.; Arham, Z. *et al.* High-Performance COD detection of organic compound pollutants using sulfurized-TiO<sub>2</sub>/Ti nanotube array photoelectrocatalyst. *Electrocatalysis* **13**, 580-589 (2022).
  - 32) Maulidiyah, M.; Wibowo, D.; Herlin, H.; Andarini, M.L.; Ruslan, R.; Nurdin, M. Plasmon enhanced by Ag-doped S-TiO<sub>2</sub>/Ti electrode as highly effective photoelectrocatalyst for degradation of methylene blue. *Asian J. Chem.* **29**, 2504-2508 (2017).

---

CC BY-SA 4.0 (Attribution-ShareAlike 4.0 International). This license allows users to share and adapt an article, even commercially, as long as appropriate credit is given and the distribution of derivative works is under the same license as the original. That is, this license lets others copy, distribute, modify and reproduce the Article, provided the original source and Authors are credited under the same license as the original.

